SENSITIVITY OF THE DDM PEAK TO GEOPHYSICAL VARIABLES

A. Camps[1], H. Park[2]
[1]Dept. of Signal Theory and Communications, Universitat Politècnica de Catalunya
[1]Dept. of Physics, Universitat Politècnica de Catalunya
CommSensLab-UPC and IEEC/CTE-UPC,
Universitat Politècnica de Catalunya - Campus Nord, E-08034 Barcelona, Spain
E-mail: adriano.jose.camps@upc.edu

ABSTRACT

GNSS-R (Global Navigation Satellite Systems Reflectometry) can be understood as a multi-static radar with as many transmitters as navigation satellites and in view and can be tracked. GNSS-Reflectometers can process the reflected signals as a scatterometer, as an altimeter, or as an unfocused synthetic aperture radar. GNSS-R has demonstrated its potential to infer numerous geophysical variables over land (soil moisture, vegetation height, detecting freeze-thaw states…), over the ocean (wind speed and direction, significant wave height, sea surface altimetry…), over sea ice (extent, depth, type…). Even a marine plastics litter product has been recently released by NASA, and some have suggested that sea surface salinity could also be inferred. In scatterometric applications the most widely used GNSS-R observable is the peak of the Delay Doppler Map (DDM), and many efforts have been directed towards an accurate instrument calibration. However, many geophysical parameter retrievals have neglected some variations of the DDM linked to the observation geometry, as well as the sensitivity to other geophysical variables. In this study we present analyze some of these effects and present a sensitivity analysis for the ocean case, notably the impact of the wind direction (WD), the 10 m height wind speed (U_{10}), which is routinely obtained today from GNSS-R observables, the sea surface temperature (SST) and sea surface salinity (SSS), and the presence of oil slicks. This quantitative study illustrates the challenges presented to retrieve some of these variables, the required corrections and their accuracy.

Index Terms— GNSS-R, sensitivity, geophysical variables

1. INTRODUCTION

The most generic GNSS-R observable is the "Delay Doppler Map," which can be obtained from the cross-correlation for different delays and Doppler frequency shifts of the reflected signal and either a locally-generated replica of the transmitted signal in the so-called "conventional" GNSS-R, or with the direct signal itself in the so-called "interferometric" GNSS-R. The cut in the time domain (constant Doppler frequency) of the DDM along its peak is called the "Waveform" (WF). Over the ocean, the DDM has a "boomerang" shape, which -general- is not symmetric, and depends on the relative velocity vectors of the transmitter and receiver (α_T and α_R angles in Fig. 1, adapted from [1]).

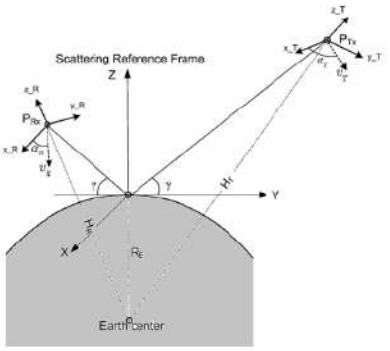

Fig. 1. Scattering reference frame of GNSS-R observation arrangement is used in the simulation [1].

The length of the tails of the DDM, and the trailing edge of the WF are most sensitive to the mean squared slope (mss), which -over the ocean- can be related to the wind speed, and increase for larger mss, as scattering comes from a larger area (i.e. larger range of delays and Doppler frequencies). The peak of the DDM (or the WF) is also sensitive to the mss, but it is most sensitive to the dielectric constant through the scattering coefficient. These properties are used to infer e.g. wind speed over the ocean (e.g. [2]), or soil moisture over land (e.g. [3,4]).

In many geophysical retrieval algorithms only the dependence of the DDM or WF peak, or the reflection coefficient (bistatic radar cross-section to be more precise), with the incidence angle is considered. In this study, we analyze the dependence of the DDM peak on the α_T and α_R angles, the wind direction, as well the sea surface temperature and salinity, and the presence of oil slicks.

2. MATERIALS AND METHODS

In order to do that, the general formulation that relates the instrument, observation geometry, and scene parameters is used (eqn. (27) of [5]), as implemented in [6,7]. The Cox and Munk model for the mss as a function of the wind speed [8], with the modifications introduced by Katzberg et al. (eqns. 3 and 4 of [9]).

DOI: 10.1109/IGARSS46834.2022.9883858

In all the following simulations, the following parameters have been used, unless otherwise stated GPS L1 C/A signal, 1 ms coherent integration time, 1 s incoherent integration time, DDMs computed in 100 x 50 Hz Doppler frequency bins times 100 x 0.1 C/A chips in delay, α_T and α_R angles equal to 0°, receiver height equal to 500 km, SST equal to 19°C, SSS equal to 35 psu, $\phi_{U10} = 0°$, receiver's bandwidth equal to 2 MHz, and noise free conditions.
For all scanned variables, results are normalized to the DDM peak of the first value, except for the impact of oil spills, in which they are normalized to the clean water case.

3. RESULTS

3.1. Impact of the relative speed vectors

The impact of the α_T and α_R angles is presented in Fig. 2. The angle α_R is set to 0°, while α_T is varied over 360°. Simulations are conducted for two wind speeds (5 and 15 m/s), and three elevation angles (15°, 45°, and 75°). As it can be appreciated, the variations exhibit a quasi-sinusoidal behavior with α_T, and decrease with increasing wind speed, and increasing elevation angle (θ_e). In any case, the largest DDM peak change is $< 10^{-4}$ dB, so it is negligible to all effects, and we can focus on the DDM peak variations with θ_e.

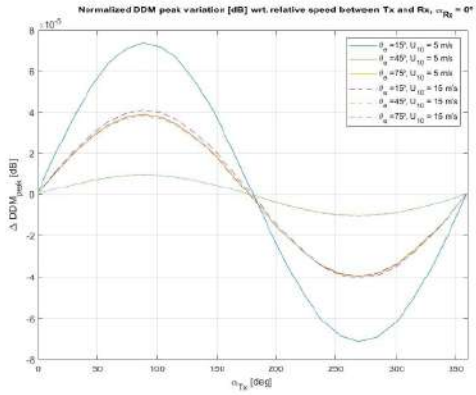

Fig. 2. DDM peak changes due to relative speed vectors.

3.2. Impact of wind speed and direction

The impact of the wind speed (U_{10}) and direction (WD) is presented in Fig. 3. As it is well known, and exploited to infer wind speed, the peak of the DDM rapidly decreases ~4.5 dB when the U_{10} increases from 2.5 to ~30 m/s. Note that the model is not including the presence of sea foam, so further reflectivity decreases should be expected if included. The dependence with the incidence angles is small (≤0.5 dB), but not negligible, at the largest U_{10} and elevation angles. The wind direction impact is negligible, with peak values ≤0.01 dB at the largest and smallest elevation angles.

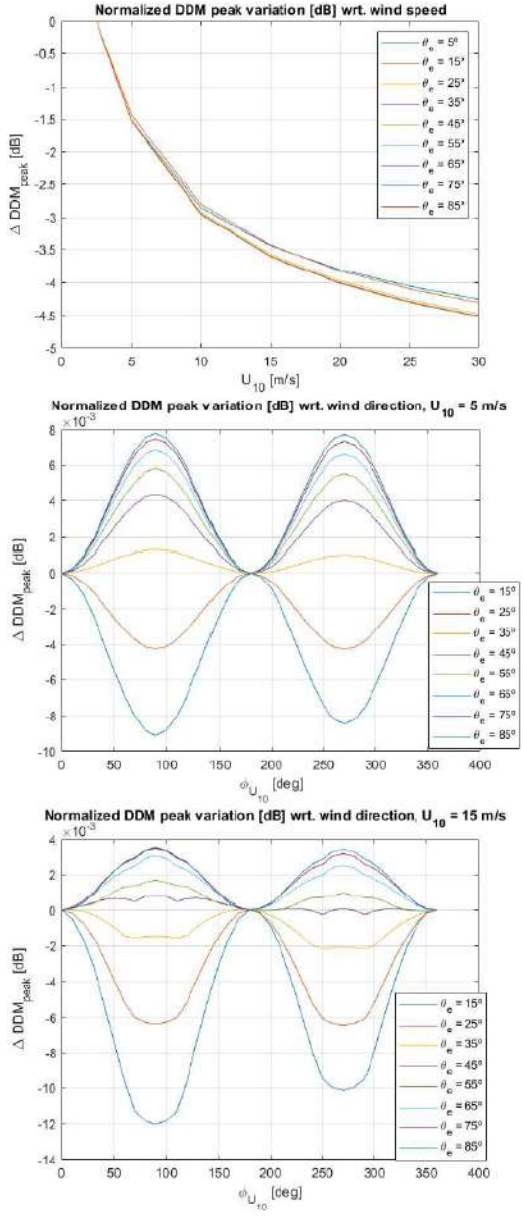

Fig. 3. DDM peak changes due to wind speed (a), and wind direction for U_{10} = 5 m/s (b), and U_{10} = 15 m/s.

3.3. Impact of Sea Surface Temperature

The impact of the Sea Surface Temperature (SST) is presented in Fig. 4. At ~20°C a non-negligible 0.2-0.3 dB error is induced, depending on the elevation angle, which almost doubles at ~30°C, the maximum SST in the oceans. This is an important error term, but it can be easily taken into account using auxiliary data.

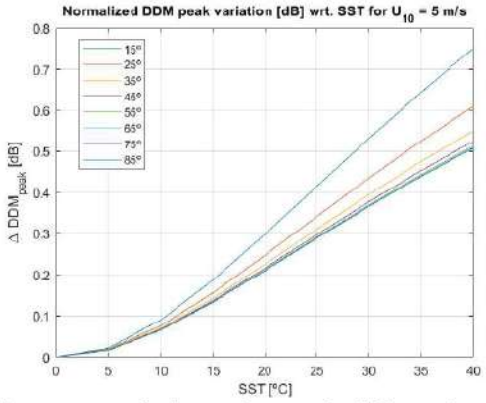

Fig. 4. DDM peak changes due SST for different elevation angles, at U_{10} = 5 m/s.

3.4. Impact of Sea Surface Salinity

The impact of the Sea Surface Salinity (SSS) is presented in Fig. 5. The largest DDM variation occurs from 25 to 30 psu, with a very small peak variation <0.05 dB, while at 35 psu (average SSS in the oceans) the absolute DDM variation ranges from 0.02 to 0.04 dB, depending on the incidence angle. The largest DDM peak sensitivity to SSS is then ~0.002 dB/psu.

If the most relaxed oceanographic requirement for ocean salinity demands a 0.1 psu uncertainty, with a horizontal resolution of 1000 km, every 30 days [10], it would still be a challenge to derive SSS from GNSS-R observations as, at best, the reflectivity error could be reduced by a factor ~150 (squared root of the number of independent observations).

In any case, it has already been proven that the combination of GNSS-R and L-band microwave radiometry data can produce single-pass SSS retrievals with a 0.43 psu error [11].

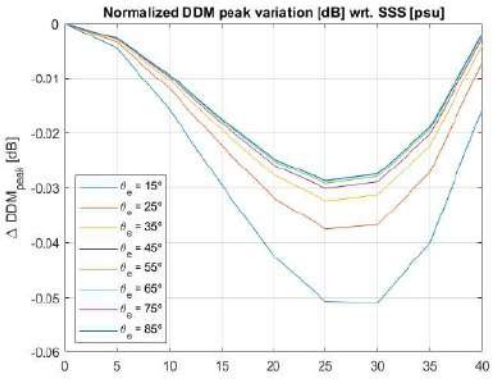

Fig. 5. DDM peak changes due SSS for different elevation angles, at U_{10} = 5 m/s or 15 m/s (no difference).

3.5. Impact of the presence of oil spills

The impact of the presence of oil spills is presented in Fig. 6. The lines represent the increase in the DDM peak due to the presence of oil, with respect to the DDM computed for the same U_{10}, SSS and SST in clean water. It is worth noting the very significant increase of the DDM peak due to the damping of the capillary waves, which produces a stronger forward scattering. When comparing these results to Fig. 3a, for example at U_{10} = 15 m/s, the effect of the wind was a decrease of ~3.5 dB wrt. to U_{10} = 2.5 m/s, while now, due to the presence of the oil spill, increases it by ~2.5 dB (~3.7 dB – 1.2 dB), so the net DDM peak decrease will be just ~1 dB.

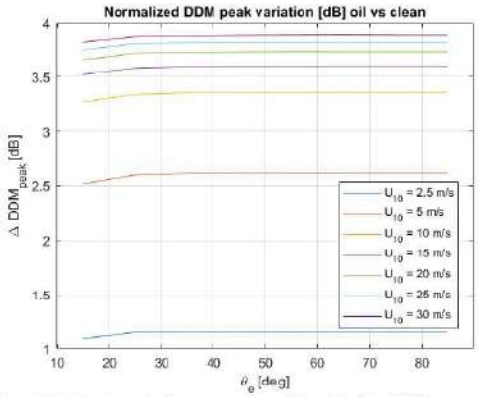

Fig. 6. DDM peak changes due oil spills for different elevation angles, and wind speeds.

4. CONCLUSIONS

This study has analyzed the sensitivity of the peak of the DDM over the ocean to the relative speed vectors between transmitter and receiver, wind speed and direction, sea surface temperature and salinity, and the presence of oil slicks. Among all these factors, as expected, the largest impact is given by the wind speed which decreases the DDM peak by up to 4-4.5 dB at 30 m/s, but larger reductions are expected if the model had included the sea foam. Oil spills damp the capillary waves, and increase the forward scattering, compensating to a large extent the decrease induced by the wind-driven roughness. Sea surface temperature has also a non-negligible effect, but it can be easily corrected for using auxiliary data.

NASA recently announced a CYGNSS Ocean Microplastic product [12]. As stated "microplastic concentration number density (#/km2) is estimated by an empirical relationship between ocean surface roughness and wind speed," but "user caution is advised in regions containing independent, non-correlative factors affecting ocean surface roughness, such as anomalous atmospheric conditions within the Intertropical Convergence Zone, biogenic surfactants (such as algal blooms), oil spills, etc."

Therefore, if the presence of oil spills can be detected by other means (e.g. [14]), its impact in the mss could be estimated and the DDM peak value corrected, thus improving the estimates of e.g. wind speed and microplastic products.

5. ACKNOWLEDGEMENTS

This work was (partially) sponsored by project SPOT: Sensing with Pioneering Opportunistic Techniques grant RTI2018-099008-B-C21/AEI/10.13039/501100011033.

6. REFERENCES

[1] H. Park, A. Camps, E. Valencia, et al. "Retracking considerations in spaceborne GNSS-R altimetry," GPS Solut 16, 507–518 (2012). https://doi.org/10.1007/s10291-011-0251-7

[2] G. Foti, C. Gommenginger, P. Jales, M. Unwin, A. Shaw, C. Robertson, and J. Roselló, "Spaceborne GNSS reflectometry for ocean winds: First results from the UK TechDemoSat-1 mission," Geophys. Res. Lett., 42, 5435–5441, (2015). doi:10.1002/2015GL064204.

[3] A. Camps *et al.*, "Sensitivity of GNSS-R Spaceborne Observations to Soil Moisture and Vegetation," in *IEEE Journal of Selected Topics in Applied Earth Observations and Remote Sensing*, vol. 9, no. 10, pp. 4730-4742, Oct. 2016, doi: 10.1109/JSTARS.2016.2588467.

[4] C. Chew, R. Shah, C. Zuffada, G. Hajj,D. Masters, and A. J. Mannucci, "Demonstrating soil moisture remote sensing with observations from the UK TechDemoSat-1 satellite mission," Geophys. Res. Lett.,43, 3317–3324, (2016), doi:10.1002/2016GL068189.

[5] V. U. Zavorotny and A. G. Voronovich, "Scattering of GPS signals from the ocean with wind remote sensing application," in *IEEE Transactions on Geoscience and Remote Sensing*, vol. 38, no. 2, pp. 951-964, March 2000, doi: 10.1109/36.841977.

[6] H. Park *et al.*, "A Generic Level 1 Simulator for Spaceborne GNSS-R Missions and Application to GEROS-ISS Ocean Reflectometry," in *IEEE Journal of Selected Topics in Applied Earth Observations and Remote Sensing*, vol. 10, no. 10, pp. 4645-4659, Oct. 2017, doi: 10.1109/JSTARS.2017.2720625.

[7] H. Park, A. Camps, J. Castellvi and J. Muro, "Generic Performance Simulator of Spaceborne GNSS-Reflectometer for Land Applications," in *IEEE Journal of Selected Topics in Applied Earth Observations and Remote Sensing*, vol. 13, pp. 3179-3191, 2020, doi: 10.1109/JSTARS.2020.3000391.

[8] C.S. Cox, and W. Munk, "Measurement of the roughness of the seasurface from photographs of the sun's glitter," J. Opt. Soc. Am.,44, (1954), pp. 838–850.

[9] S.J. Katzberg, O., Torres, and G. Ganoe, "Calibration of reflected GPS for tropical storm wind speed retrievals," Geophys. Res. Lett., 33, L18602, (2006), doi:10.1029/2006GL026825.

[10] World Meteorological Organization – OSCAR: Observing Systems Capability Analysis and Review Tool https://space.oscar.wmo.int/requirements/view/504 (last visited January 10th, 2022)

[11] J.F. Munoz-Martin, and A. Camps, "Sea Surface Salinity and Wind Speed Retrievals Using GNSS-R and L-Band Microwave Radiometry Data from FMPL-2 Onboard the FSSCat Mission." *Remote Sens.* **2021**, *13*, 3224. https://doi.org/10.3390/rs13163224

[12] CYGNSS Ocean Microplastic Concentration (Version 1.0) Release: https://podaac.jpl.nasa.gov/announcements/2021-11-24-CYGNSS-Ocean-Microplastic-Concentration-V1.0-Release (last visited January 10th, 2022)

[13] M.C. Evans, and C.S. Ruf, "Toward the Detection and Imaging of Ocean Microplastics with a Spaceborne Radar," IEEE Transactions on Geoscience and Remote Sensing, http://doi.org/10.1109/TGRS.2021.3081691

[14] M. Fingas, and C.E. Brown, "A Review of Oil Spill Remote Sensing." Sensors 2018, 18, 91. https://doi.org/10.3390/s18010091